

the nuclei examined are not deformed, but are essentially spherical in shape.

ACKNOWLEDGMENTS

The authors wish to express their thanks to the operating crew, electronic maintenance crew, and to the

mechanical technicians, for their cooperation during the experiment. They are also grateful to Dr. G. Rogosa and the AEC Cross Section Isotopes Pool for loan of the enriched isotopes. Finally, they wish to acknowledge theoretical help given by Dr. F. Buskirk of the Naval Post Graduate School at Monterey.

Polarization of Neutrons from the $N^{14}(d,n_0)O^{15}$ Reaction*

H. M. EPSTEIN,† D. F. HERRING,‡ AND K. W. JONES§

The Ohio State University, Columbus, Ohio

(Received 18 May 1964)

The polarization of neutrons from the $N^{14}(d,n_0)O^{15}$ reaction has been measured at 1.32 MeV for laboratory angles from 0 to 90 deg. The polarization is positive (using the Basel sign convention) and has a maximum value of about 0.10 at 30 deg. The neutrons were produced by bombardment of a 220-keV-thick nitrogen gas target with deuterons from The Ohio State University electrostatic accelerator. The polarization of the neutrons was determined by a measurement of the left-right asymmetry in the scattering of the neutrons from a liquid-helium scintillation counter. Time-of-flight and pulse-shape discrimination techniques were used to reduce the background. Compound nucleus and distorted-wave Born-approximation direct interaction calculations were carried out and compared with the polarization data as well as with the available differential cross-section measurements.

1. INTRODUCTION

A MEASUREMENT of the polarization of the neutrons from the $N^{14}(d,n_0)O^{15}$ reaction at low energies is of interest for several reasons. The interaction mechanism for the $N^{14}(d,n_0)O^{15}$ reaction and the mirror reaction $N^{14}(d,p_0)N^{15}$ is uncertain at bombarding energies below 2 MeV. The excitation curves, particularly for the $N^{14}(d,n_0)O^{15}$ reaction, show peaks which can be correlated with states in the O^{16} compound nucleus measured by other means. The angular distributions have been interpreted as evidence for a few-level compound nucleus reaction¹ and for plane-wave exchange stripping.^{2,3} The addition of polarization data might help to distinguish between the compound nucleus and stripping interaction mechanisms.

If the reaction should proceed in large part by compound nucleus formation, it might also be possible to extract the parameters of the compound states involved. For deuteron bombarding energies around 2-MeV states in O^{16} around 22.7 MeV would be excited. This excitation energy is near that of the giant dipole resonance observed in the photodisintegration of O^{16} . The properties of the giant dipole state have recently

been of considerable theoretical interest,⁴ and additional experimental knowledge of the parameters of the excited states in this energy region should be useful.

The $N^{14}(d,n_0)O^{15}$ reaction has been used as a source of neutrons of energies around 6 MeV. It is not as convenient a source of neutrons as the $D(d,n)He^3$ or the $T(p,n)He^3$ reactions because of its substantially lower cross section and the lower energy neutrons produced in the $N^{14}(d,n)O^{15}$ reactions and the gamma rays resulting from the (d,n) , (d,p) , and (d,α) reactions. However, if the neutrons from the $N^{14}(d,n_0)O^{15}$ reaction are highly polarized, the reaction might still be of interest as a source of polarized neutrons.

2. EXPERIMENTAL METHOD

The neutrons from the $N^{14}(d,n_0)O^{15}$ reaction were produced by bombardment of a N^{14} gas target with deuterons from The Ohio State University electrostatic accelerator. The gas target was a 0.010-in. stainless steel tube with a tantalum beam stop and a 1.27- μ nickel entrance foil. The target length was 1.2 cm and the target pressure 0.5 atm. The energy loss of the beam in traversing the target gas filling was about 220 keV. The resulting average beam energy was 1.32 MeV. Beam currents of about 0.7 μ A were used. It was originally planned to make measurements on the peak in the zero-degree excitation curve at 1.5 MeV, but this was impossible because of limitations in accelerator performance. The 1.32-MeV energy actually

* Work supported in part by the U. S. Atomic Energy Commission and The Ohio State University Development Fund.

† Supported by Battelle Memorial Institute fellowship. Present address: Battelle Memorial Institute, Columbus, Ohio.

‡ Present address: General Atomic, San Diego, California.

§ Present address: Brookhaven National Laboratory, Upton, New York.

¹ W. M. Jones, Nucl. Phys. 26, 203 (1961).

² J. L. Weil and K. W. Jones, Phys. Rev. 112, 1975 (1958).

³ T. Retz-Schmidt and J. L. Weil, Phys. Rev. 119, 1079 (1960).

⁴ See, for example, G. E. Brown, L. Castillejo, and J. A. Evans, Nucl. Phys. 22, 1 (1961).

used represents the highest energy that could be achieved with reliable operation of the accelerator over long periods of time.

The polarization of the neutrons was determined by a measurement of the left-right asymmetry in scattering from a sample of liquid helium. Helium is a convenient polarization analyzer for the approximately 6-MeV neutrons considered here because the scattering cross section is high, and the scattering phase shifts from which the analyzing strength is computed are fairly well known and change slowly with energy. The use of liquid helium provides a straightforward way of obtaining a high-density sample. The asymmetry measurements were made for neutrons scattered by the helium sample at an angle of 65° in the laboratory system. This angle corresponds to a peak in the polarization angular distribution and combines a high polarization of about 0.7 with a reasonable scattering cross section. The polarization is close to 1.0 at back angles, but the scattering cross section is also substantially lower than at the forward angles.

The major problem in a double scattering experiment is to achieve a good signal-to-background ratio. This is particularly difficult to do for the $N^{14}(d,n_0)O^{15}$ reaction, since the gamma background is high and the cross section is a maximum of 2.2 mb/sr at this energy. In addition to providing a shield between source and final detector, it was necessary to use the liquid helium as a scintillation counter to detect the recoil alpha particle produced by the scattered neutron so that the neutron time-of-flight between the liquid-helium Dewar and final detector could be measured. This procedure eliminated effects of shield penetration, scattering from the walls of the Dewar, and room background. However, the bombardment of N^{14} produces copious quantities of ener-

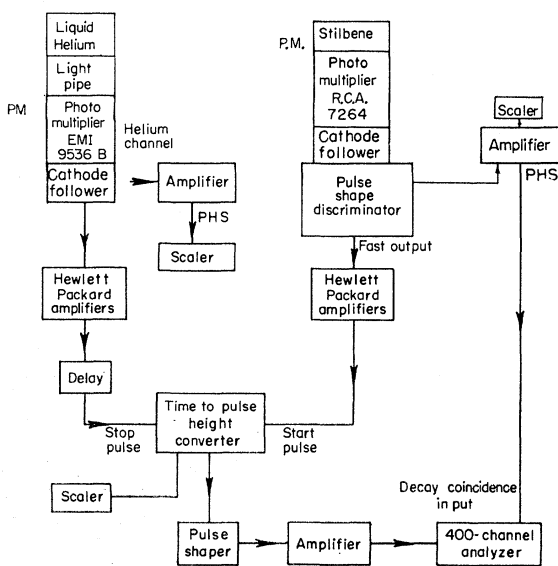


FIG. 1. Block diagram of electronics.

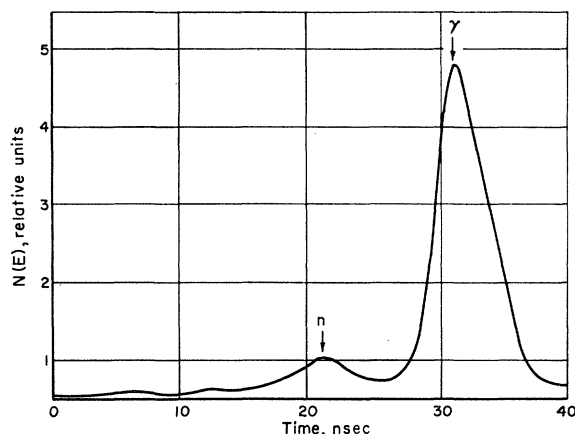


FIG. 2. Time-of-flight spectrum, without pulse-shape discrimination, of the neutrons from the reaction $N^{14}(d,n_0)O^{15}$. A flight path of 22 cm was used.

getic gamma rays from the various (d,p) , (d,n) , and (d,α) reactions. The energy deposited in the helium scintillation counter by the recoil alphas from scattered neutrons and by Compton electrons from scattered gamma rays is almost the same. The time-of-flight measurement used a rather short flight path to obtain the maximum possible counting rate and hence, the neutron and gamma-ray peaks were not well resolved. The gamma-ray peak in the time-of-flight spectrum was eliminated by using a pulse-shape discrimination circuit on the final scintillation detector.

The various components of the experimental apparatus are discussed in more detail in the following sections.

2.1. Electronics

A block diagram of the electronics is shown in Fig. 1. An EMI 9536-B phototube was used to view the liquid-helium scintillator. Faster tubes such as the RCA 7264, 7746, and 6810A were also tried, but were found to be unsatisfactory because of high-noise levels. The pulse heights from the stilbene neutron detector were much larger and an RCA 7264 was used successfully. A standard Eldorado model TH-300 time-to-pulse-height converter was used for the time-of-flight measurement. The pulse-shape discrimination circuit was that described by Daehnick and Sherr.⁵ No attempt was made to use pulse-height selection on slow side channels because of the loss of counting efficiency.

The over-all time resolution of the system averaged 7 nsec over the course of the experiment. Figure 2 shows a time-of-flight spectrum without gating of the multi-channel analyzer by the pulse-shape discriminator. Figure 3 shows a typical time-of-flight spectrum obtained when the analyzer was gated by the pulse-shape discriminator. A flight path of 22 cm was used. A

⁵ W. E. Daehnick and R. Sherr, Rev. Sci. Instr. **32**, 666 (1961).

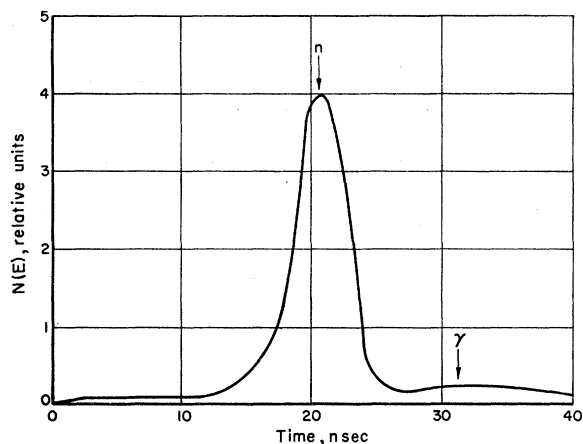


FIG. 3. Time-of-flight spectrum, with pulse-shape discrimination, of the neutrons from the reaction $N^{14}(d, n_0)O^{16}$. A flight path of 22 cm was used.

comparison of the two spectra demonstrates the effectiveness of the pulse shape discriminator in rejecting the scattered gamma rays.

2.2. Liquid-Helium Dewar

The liquid-helium Dewar used in the experiment is shown in Fig. 4. The design of the Dewar is very similar to that used by Baicker and Jones.⁶ The major change made was to increase the size of the central filling tube so that a light pipe could be used to transmit light from the helium scintillator to the phototube, which was at room temperature. The liquid-helium loss rate for the system was about 0.1 l/h. One filling of the Dewar was sufficient for 20 h of operation.

The light pipe used was a Lucite cylinder 1 in. in diameter and 33 in. long. The light transmission of the pipe was determined by a measurement of the pulse height produced by an alpha source and CsI(Tl) crystal mounted successively on the end of the pipe and directly on the phototube. The transmission measured in this way was about 0.15.

The scintillating volume was defined by a cylindrical cell at the end of the light pipe 1.125 in. in diameter and 2.75 in. long with a wall thickness of 0.020 in. The surface of the cell was painted with white Tygon paint as a reflector⁷ after first thoroughly cleaning the surfaces with nitric acid and acetone. A thick coating of diphenyl stilbene (DPS) wavelength shifter about 150 mg/cm² thick was then vacuum evaporated over the Tygon paint. DPS films from 0 to 100 mg/cm² were also tried on the end of the light pipe, but the largest pulse heights were obtained with no wavelength shifter at all.

The resolution of the helium scintillator was measured with an alpha source immersed in the liquid

helium and was about 34%. The light collection efficiency in the cell as a function of the position of the light source was measured with an alpha source mounted on a CsI(Tl) crystal at room temperature. Pulse heights changed by a factor of two when the source was moved from the top to the bottom of the cell. The resolution for recoil alphas from 4.5-MeV neutrons scattered at 80° was measured by gating the multichannel analyzer with the signal from the final neutron detector. The resolution was then somewhat worse than with the alpha source because of the variation of cell response with scintillation position.

In the present experiment, approximately 6-MeV neutrons were scattered from the helium at an angle of 65°. The resulting recoil alpha particle has an energy of about 1.5 MeV. A 5-MeV gamma ray undergoing a Compton scatter in the reaction plane at 65° produces a recoil electron which can lose up to 1 MeV of energy in the cell. No pulse-height selection was attempted on the helium scintillator, and hence both neutrons and gamma rays contributed to the ungated time-of-flight spectrum.

2.3. Final Detector

The neutrons scattered by the liquid helium were detected in a 3-in.-long by 2-in.-diam stilbene crystal. The calculated total detection efficiency for neutrons incident on this crystal was about 40%. Stilbene was

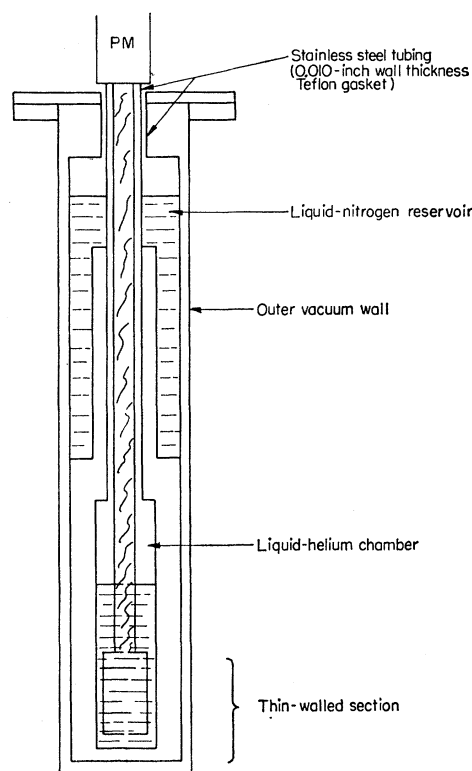


FIG. 4. Liquid-helium Dewar and scintillation counter.

⁶ J. A. Baicker and K. W. Jones, Nucl. Phys. 17, 424 (1960).

⁷ J. E. Simmons and R. B. Perkins, Rev. Sci. Instr. 32, 1173 (1961).

chosen for the final neutron detector because of its high efficiency for decay-time discrimination. The detector was placed at the center of a cylindrical shield 2 ft in diameter and 8 in. thick with a 2-in. hole along a diameter for the neutron beam and detector electronics. The shield was composed of an equal mixture of steel and borated paraffin. It gave a minimum attenuation of about 100 for 6-MeV neutrons and 20 for 6-MeV gammas. The size of the shield prevented the taking of data at angles greater than 90° with respect to the incident beam.

2.4. Experimental Checks on Equipment

The performance and alignment of the equipment was checked by measuring the left-right (L-R) scattering asymmetry for neutrons emitted at 0° to the incident deuteron beam. The values obtained during the experiment were 1.00 to within the counting statistics of $\pm 3\%$. Polarization measurements were also made on both sides of the incident deuteron beam at angles less than 40° in order to eliminate effects of geometrical misalignments. A measurement of the polarization of neutrons from the $D(d,n)He^3$ reaction was also made at an angle of 45° at a mean deuteron energy of 1.32 MeV. The polarization value obtained was -0.14 ± 0.03 (Basel convention) which is in reasonable agreement with past results.⁸

3. ESTIMATE OF ERRORS AND UNCERTAINTIES

Polarization measurements, while simple in principle, are actually rather difficult in practice. For this reason the possible errors in the experiment are discussed here in some detail.

3.1. Statistical Uncertainties

Counting statistics were a major limitation to the experimental accuracy because of the very low neutron intensities in this experiment.

Because random background can show no time correlation, the background evaluation made use of the time-of-flight spectrum. Counts in those channels not near the neutron peak were averaged to give a background count per channel which was then subtracted from the channels covered by the neutron peak. Statistical uncertainties in the difference or ratio between two quantities were calculated in the usual way. The signal-to-background ratio was strongly dependent on the neutron production cross section and the position of the final detector relative to the incident deuteron beam. The ratio varied from about 20 to 1.5.

3.2. Uncertainty in the Value of θ_1

For the reaction considered, the polarization appears to vary slowly with θ_1 , the angle between the incident

deuteron beam and the outgoing neutron produced in the $N^{14}(d,n_0)O^{15}$ reaction, such that the maximum uncertainty of 1.5° in θ_1 introduces an error of less than 1% in the measured polarization.

3.3. Uncertainty in the Value of θ_2

The counting rate is extremely sensitive to the value of θ_2 , the scattering angle of the neutrons from the liquid-helium sample, because of the rapid variation of the $He^4(n,n)He^4$ cross section with angle. Rather elaborate techniques were therefore used to set this angle. The entire shield and detector were rotated about the geometrical center of the helium scatterer on precision bearings. The angle θ_2 was read from a vernier dial to 0.1° . The zero position of θ_2 was determined by both optical sighting and by finding the center of symmetry in the angular distribution about θ_2 of neutrons scattered from the helium Dewar, with θ_1 set at 0° . These two calibration methods agreed to within $\pm 0.2^\circ$. Good agreement between the left-right symmetries for $\pm\theta_1$ measured at several points indicate that there should be no large systematic error in θ_2 . An error of 0.2° in θ_2 gives a maximum error of 0.8% in the polarization.

3.4. Asymmetries in the Helium Container

It was found that asymmetries in the helium Dewar could cause variation of about $\pm 0.4^\circ$ in θ_2 if the Dewar position was changed. However, this effect was essentially eliminated by keeping the Dewar in a fixed position and performing the calibrations listed in the preceding paragraph with the Dewar in this position.

3.5. Photomultiplier Gain Shifts

A magnetic shield around the photomultiplier essentially eliminated drifts in gain from stray magnetic fields. The counting rate from a gamma-ray source, for several positions of the detector collimator, varied by less than 1%. The dependence of the photomultiplier gain on counting rate was checked carefully. No observable effect was found for the rates encountered in this experiment. Any effect was also minimized during the experiment by requiring the same number of counts (to within 1%) from the photomultiplier viewing the liquid-helium sample for each of the sequence of runs necessary to obtain a L-R ratio.

3.6. Neutron Flux Contamination

The presence of extraneous neutron groups from excited state reactions or contaminant reactions could seriously affect the results. However, neutrons to the first excited state of O^{15} are emitted with an energy of about 1 MeV and would have little likelihood of exceeding the bias set on the liquid-helium cell by the time-to-pulse-height converter stop pulse requirements. No lower energy neutron group was observed in the time-of-flight spectrum.

⁸ W. Haeblerli, in Proceedings of the International Symposium on Polarization Phenomena of Nucleons, Basel, July 1960 (unpublished); *Helv. Phys. Acta*, Suppl. 6, 149 (1961).

The possibility of deuterium, nitrogen, or carbon contamination of the foil or the end cap of the gas target was also considered. Backgrounds, which were taken with helium replacing nitrogen in the target, showed only the presence of a very small peak due to $N^{14}(d, n_0)$ neutrons, representing about 15% of the $N^{14}(d, n_0)$ neutrons with the target filled. The background is probably caused by nitriding of the beam stop and nickel foil. This type of background should not appreciably affect the measured polarization.

3.7. Finite Geometry Effects

The equation,

$$P_1(\theta_1)P_2(\theta_2) = (R/L - 1)/(R/L + 1),$$

where $P_1(\theta_1)$ is the reaction polarization, $P_2(\theta_2)$ is the analyzer polarization, R is the count rate of detector at θ_2 (Basel convention), and L is the count rate of detector at $-\theta_2$ (Basel convention), which gives the polarization in terms of the measured L/R asymmetry is derived on the assumption that the scatterer and detector are infinitesimally small. Thus, the scattering plane is identical with the nuclear reaction plane. In any real experiment these conditions can only be approximated. In this experiment, the scatterer is a cylinder 6.35 cm long by 2.86 cm in diameter, and the detector is 7.62 cm long by 5.08 cm in diameter. The distance between source and scatterer and detector was 21.6 cm. The correction for scattering out of the reaction plane causes a decrease in P_2 of about 1%. Since P_2 is not known to better than $\pm 5\%$, this correction is negligible. It does not affect the asymmetry ratio L/R. However, any shift in the effective center of the scatterer in the reaction plane will lead to a false asymmetry. Variations of neutron production and scattering cross sections with angle produce a larger flux on one side of the scatterer and detector than the other, causing the effective center to shift. The shift of the effective center for the present experiment was evaluated by means of the known cross sections. The shift in the helium cell effective center led to a maximum false asymmetry of 0.1%. The shift in the effective center of the final detector changed θ_2 by about 0.5° . However, this deviation introduces no false asymmetries. It merely alters the analyzing angle by a negligible amount. Both of these effects, as well as the variation of helium polarization over the angle subtended by the counter, were taken into account during the calculation of the polarization.

3.8. Multiple Scattering

Since the mean free path for a 6-MeV neutron in liquid helium is 29 cm, the effect of multiple scattering in the 1.43-cm-radius helium cell should be negligible. However, effects are possible due to scattering events occurring in materials outside the cell. It is, therefore,

necessary to consider how multiple scattering affects the experimental results. To a good approximation, second scatter loss of neutrons which are headed for the detector will have no effect on the asymmetry ratio L/R because the fraction of neutrons scattered out should be almost the same for the left and right experiment. It is the neutrons scattered into the detector which are of concern. Pulses from those neutrons scattered into the detector which were not first scattered in the liquid-helium scintillator cell will be eliminated by the time-of-flight measurement. Those neutrons which make a strongly forward-angle scatter in the helium cell cannot produce a large enough helium recoil pulse to overcome the helium channel bias, about a 0.5-MeV helium recoil is required, unless the second scatter is also in the cell. Since the helium cross section strongly favors small angle scattering the latter requirement greatly limits the "in scattering" events. It is estimated that with the above limitation, the relative error due to multiple scattering is approximately $\Delta P/P \approx 5\%$. To correct for this error it would be necessary to slightly increase the polarization values.

3.9. Collimator Effects

The iron-paraffin collimator surrounding the detector was responsible for some neutron "in scattering." The use of paraffin in the collimator, of course, tended to minimize this effect because of the very low albedo of this material to fast neutrons. Actually, the only effect of the collimator scattering is to increase the effective solid angle subtended by the detector. Since it has been shown that the finite geometry corrections are negligible for the detector, this is not considered to be an important factor.

3.10. Uncertainties in the (He^4+n) Phases

The angular distribution of neutrons scattered by helium has been studied in a number of experiments.⁹⁻¹⁹ Although discrepancies still exist in the phase shifts below 3 MeV and, at high energies, the various results in the energy region applicable to the present experiment are in good agreement. The phase shifts actually used were those of Seagrave⁹ and were the following:

$$\delta_1^- = +48^\circ, \quad \delta_1^+ = +116^\circ, \quad \delta_0 = -60^\circ.$$

⁹ J. D. Seagrave, Phys. Rev. 92, 1222 (1953).

¹⁰ R. K. Adair, Phys. Rev. 86, 155 (1952).

¹¹ F. Demanins, G. Pisent, G. Poiani, and C. Villi, Phys. Rev. 125, 318 (1962).

¹² P. Huber and E. Baldinger, Helv. Phys. Acta 25, 435 (1952).

¹³ G. Pisent and A. M. Sarais, Nuovo Cimento 28, 600 (1963).

¹⁴ P. Marin and C. R. Banz, Compt. Rend. 248, 1316 (1959).

¹⁵ C. Schwartz, Phys. Rev. 85, 73 (1952).

¹⁶ P. Tannenwald, Phys. Rev. 89, 508 (1953).

¹⁷ S. M. Austin, H. H. Barschall, and R. E. Shamu, Phys. Rev. 126, 1532 (1962).

¹⁸ T. H. May, W. Benenson, R. L. Walter, and R. Vander Maat, Bull. Am. Phys. Soc. 7, 268 (1962).

¹⁹ D. C. Dodder and J. L. Gammel, Phys. Rev. 88, 520 (1952).

The resulting polarization for a 65° laboratory scattering angle is -0.79 . The neutron energy in the experiment changes only from 5.76 to 6.26 MeV. The polarization changes slowly with energy and the single value for the polarization can be used without introducing appreciable uncertainties. Estimates of the error in polarization resulting from uncertainties in the phase shifts are not available. Baicker²⁰ has made a very crude estimate from the uncertainties given by Dodder and Gammel and finds a value for ΔP of 0.04 to 0.06.

4. RESULTS

The polarization of the neutrons from the $N^{14}(d,n_0)O^{15}$ reaction at an average deuteron energy of 1.32 MeV for laboratory angles from 0 to 90° is given in Table I. Figures 5–8 compare the experimental results with theoretical curves calculated from compound nucleus and direct interaction theories. Figures 5, 7, and 8 also include comparisons between experimental and calculated differential cross sections. The bombarding energy was fixed by the maximum reliable operating energy of the accelerator and the energy loss of the beam in the gas target materials. The geometry of the

TABLE I. Polarization of neutrons from the $N^{14}(d,n_0)O^{15}$ reaction measured in the present experiment.^a

θ_{lab}	Polarization
10°	0.055 ± 0.015
20°	0.071 ± 0.020
30°	0.106 ± 0.019
40°	0.082 ± 0.033
45°	0.079 ± 0.025
60°	0.053 ± 0.037
75°	0.037 ± 0.041
90°	0.045 ± 0.035

^a The uncertainties shown are statistical only.

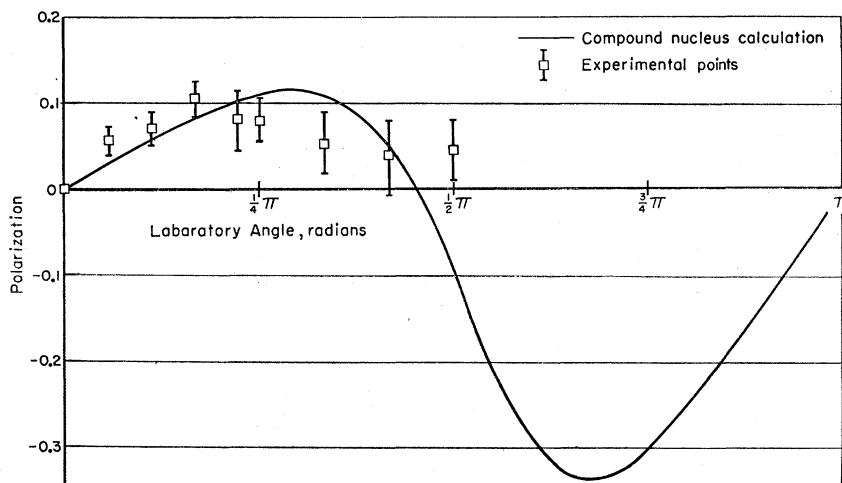


FIG. 6. Compound nucleus fit to the polarization of the neutrons from the $N^{14}(d,n_0)O^{15}$ reaction at 1.32 MeV. The parameters used in the calculation were determined by fitting the angular distribution data.

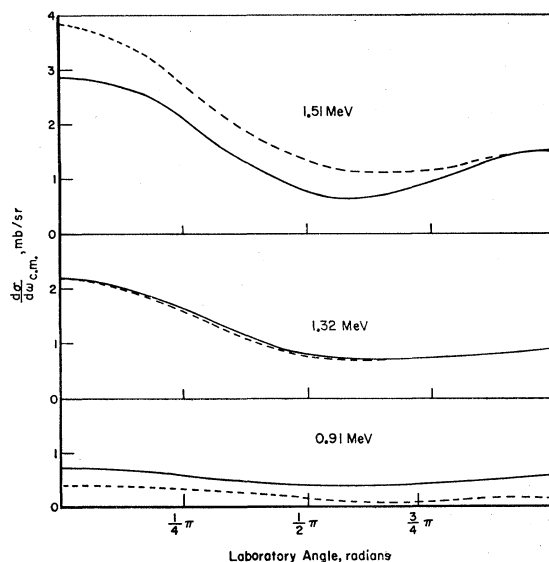


FIG. 5. Compound nucleus fits to angular distributions for the $N^{14}(d,n_0)O^{15}$ reaction at 0.91, 1.32, and 1.51 MeV. Two levels were assumed; a 1^- level at $E_d=1.6$ MeV formed by p -wave deuterons with a width of 1 MeV and a 0^+ level at $E_d=2.7$ MeV formed by s -wave deuterons with a width of 500 keV. The various partial widths and radii were adjusted to fit the angular distribution at 1.32 MeV. The solid curves are the data of Ref. 3. The distribution at 1.32 MeV was interpolated from neighboring angular distributions. The fits calculated with the above parameters are shown with a dashed line.

shielding involved prevented measurements at angles greater than 90° . The errors shown are statistical errors only.

5. ANALYSIS OF DATA

Attempts were made to fit the $N^{14}(d,n_0)O^{15}$ angular distributions around 1.32 MeV and the polarization data at 1.32 MeV on the assumption that the reaction

²⁰ J. A. Baicker, Ph.D. thesis, Columbia University, 1959 (unpublished).

takes place completely either by compound nucleus formation or by direct interaction.

The compound nucleus calculations are complex since more than one state in the compound nucleus must be considered and since both interacting particles have spin one. The direct interaction calculation must consider the distortion of the deuteron and neutron waves at these energies. A limited number of calculations were carried out using the "Sally" code of Bassel, Drisko, and Satchler.²¹

5.1. Compound Nucleus Calculations

The level structure in O^{16} from about 21- to 24-MeV excitation, corresponding to deuteron energies up to 3.7 MeV, must be considered. The available experimental information up to 15 May 1962 has been summarized by Lauritsen and Ajzenberg-Selove.²² Additional information has been provided by a number of recent experiments.²³⁻³³ Recent theoretical work has centered on the explanation of the giant resonance at 22.3-MeV excitation which dominates the photonuclear and inverse photonuclear reaction in this energy region. The giant dipole state is presumably a $T=1, 1^-$ state and would not be seen in the $N^{14}(d, n)O^{15}$ reaction if isotopic spin is conserved. Wilkinson³⁴ has estimated that, for the giant dipole resonance in O^{16} , a 10 to 50% admixture of $T=0$ is consistent with experimental data. More recently, Gillet³⁵ has shown, using the particle-hole framework, that a $T=0$ state lies very close to the $T=1$ giant dipole state. Greiner³⁶ has considered the mixing of the $T=1$ and $T=0$ states due to the Coulomb interaction and has explained the asymmetry in the (γ, n) cross sections of Firk and Lokan²⁵ and

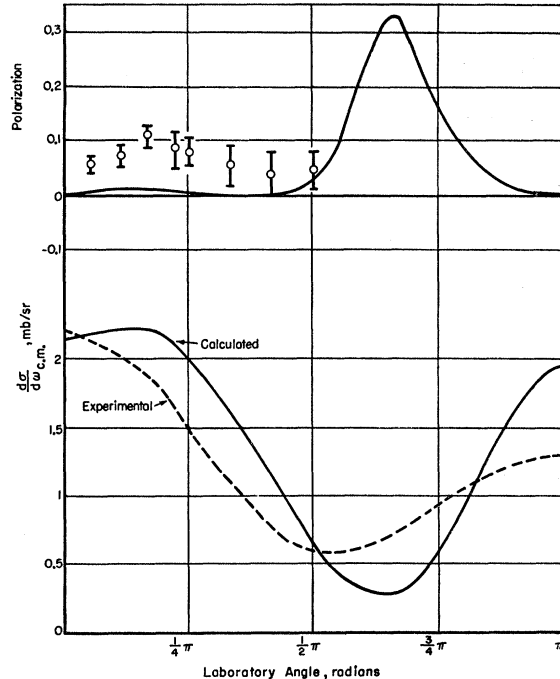


FIG. 7. Distorted-wave Born-approximation fits to the $N^{14}(d, n_0)O^{15}$ angular distribution and polarization data at 1.32 MeV. The optical model parameters used in the calculations are given in Table II. The errors shown are statistical uncertainties.

Caldwell *et al.*³⁷ as arising from the mixing and interference of these states. On the basis of these considerations, it is expected that the giant resonance might influence the $N^{14}(d, n_0)O^{15}$ reaction to some extent.

A Legendre polynomial analysis of the neutron angular distribution at 1.3 MeV shows that terms involving $P_0, P_1,$ and P_2 are required for a fit. Hence, at least two levels of opposite parity must be considered in analyzing the reaction. It was assumed that one of these levels is the 1^- level in the neighborhood of 22.1-MeV excitation. The even-parity level is assumed to lie around 23.1-MeV excitation. The assumption that the $N^{14}(d, n)O^{15}$ reaction is dominated by rather broad levels at 1.5 to 1.9 MeV and at 2.7-MeV bombarding energy is substantiated by the energy dependence of the 0° excitation curve and rather weakly by the total cross section for the reaction.³⁸ In order to form an even-parity level the l value of the incoming deuteron must be even. At a bombarding energy of 1.3 MeV, calculations show that the penetrability for $l=0$ deuterons is about 22 times that for $l=2$ deuterons. The 2.7-MeV level then must be 0^+ or 2^+ if it is assumed, on the basis of penetrabilities, to be formed by $l=0$ deuterons. The 0^+ choice gave the better fit to experi-

²¹ R. H. Bassel, R. M. Drisko, and G. R. Satchler, ORNL-3240, February 1962 (unpublished).

²² T. Lauritsen and F. Ajzenberg-Selove, Nucl. Phys. **11**, 1 (1959) and *Nuclear Data Sheets*, compiled by K. Way *et al.* (Printing and Publishing Office, National Academy of Sciences—National Research Council, Washington 25, D. C., 1961), Sets 5 and 6.

²³ R. G. Allas, T. H. Baird, L. L. Lee, Jr., and J. P. Schiffer, Bull. Am. Phys. Soc. **7**, 411 (1962).

²⁴ L. N. Bolen and W. D. Whitehead, Phys. Rev. Letters **9**, 458 (1962).

²⁵ F. W. Firk and K. H. Lokan, Phys. Rev. Letters **8**, 321 (1962).

²⁶ N. A. Burgov, G. V. Danilyan, B. S. Dolbilkin, L. E. Lazareva, and F. A. Nikolaev, Zh. Eksperim. i Teor. Fiz. **43**, 70 (1962) [English transl.: Soviet Phys.—JETP **16**, 50 (1963)].

²⁷ J. L. Weil and G. U. Din, Bull. Am. Phys. Soc. **7**, 111 (1962).

²⁸ J. Miller, G. Schuhl, G. Tamas, and C. Tzara, Phys. Letters **2**, 76 (1962).

²⁹ L. N. Bolen and W. D. Whitehead, Phys. Rev. Letters **9**, 458 (1962).

³⁰ W. R. Dodge and W. C. Barber, Phys. Rev. **127**, 1746 (1962).

³¹ R. L. Bramblett, J. T. Caldwell, and S. C. Fultz, Bull. Am. Phys. Soc. **8**, 120 (1963).

³² D. B. Isabelle and G. R. Bishop, Nucl. Phys. **45**, 209 (1963).

³³ K. N. Geller and E. G. Muirhead, Phys. Rev. Letters **11**, 371 (1963).

³⁴ D. H. Wilkinson, Phil. Mag. **1**, 379 (1956).

³⁵ V. Gillet, Ph.D. dissertation, University of Paris, 1962 (unpublished).

³⁶ W. Greiner, Nucl. Phys. **49**, 522 (1963).

³⁷ J. T. Caldwell, R. R. Harvey, R. L. Bramblett, and S. C. Fultz, Phys. Letters **6**, 213 (1963).

³⁸ N. J. Kawai, J. Phys. Soc. Japan **16**, 157 (1961).

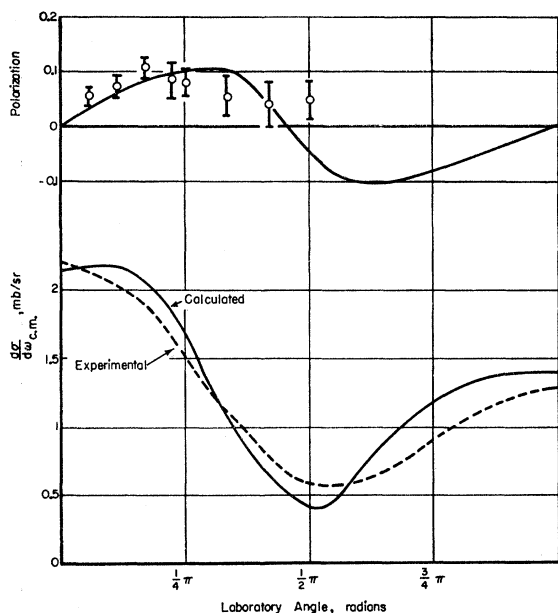


FIG. 8. Distorted-wave Born-approximation fits to the $N^{14}(d, p_0)O^{15}$ angular distribution and polarization data at 1.32 MeV. The optical model parameters used in the calculations are given in Table III. The errors shown are statistical uncertainties only.

mental data and was used for the compound-nucleus cross-section calculations.

Angular distributions were calculated by means of the formalism of Blatt and Biedenharn³⁹ and the extension by Lustig.⁴⁰ It was assumed for convenience of calculation that the phase shifts could be calculated from a single-level formula. The parameters used were chosen to give a best fit to the angular distribution at 1.32 MeV. The angular distributions are reproduced fairly well, but the fit to the energy dependence of the absolute cross section is poor. The same parameters were used to calculate the polarization from the formulas of Simon and Welton.⁴¹ The results for the cross-section calculations are shown in Fig. 5 and the results for the polarization in Fig. 6.

The compound nucleus computations described here are by no means complete. The assumption that $l < 2$ permits 12 different two-level combinations of opposite parity, and it is obvious that only a weak justification is given for the choice of the $(1^-, 0^+)$ pair. The complexity of the spin-one-on-spin-one situation makes the calculations difficult, and it is also probably not physically reasonable to assume that there are only two levels which must be considered. It does not appear, however, from the evidence considered here, that a direct interaction reaction mechanism must necessarily be invoked to explain the data.

³⁹ J. M. Blatt and L. C. Biedenharn, *Rev. Mod. Phys.* **24**, 258 (1952).

⁴⁰ H. Lustig, *Phys. Rev.* **117**, 1332 (1960).

⁴¹ A. Simon and T. A. Welton, *Phys. Rev.* **90**, 1036 (1953).

5.2. Direct Interaction Calculations

Several attempts have been made to fit the $N^{14}(d, p_0)N^{15}$ and $N^{14}(d, n_0)O^{15}$ angular distributions by plane-wave stripping⁴² or by plane-wave stripping plus exchange stripping.^{2,3} While, in some cases, a good fit can be obtained, it does not seem physically reasonable to ignore the distortion of the incoming deuteron wave at low energies. A limited number of calculations were therefore carried out using the distorted-wave Born-approximation stripping theory to see if satisfactory fits could be obtained to the angular distribution and polarization data.

The computations were carried out by use of the "Sally" program of Bassel, Drisko, and Satchler.²¹ This program does not allow for use of spin-orbit coupling and uses the zero-range approximation. Two sets of optical model parameters for the incoming deuteron were used. The parameters listed in Table II, with a real well depth of about 20 MeV, gave a good fit to the elastic scattering data of Seiler *et al.*⁴⁸ from 0.7- to 2.1-MeV bombarding energy. The parameters listed in Table III, with a real well depth of about 85 MeV,

TABLE II. Optical model parameters used for the DWBA calculations shown in Fig. 7.^a

Deuteron	Neutron
$V_0 = 21.3$ MeV	$V_0 = 43.0$ MeV
$W_0 = 4.83$ MeV	$W_0 = 6.45$ MeV
$r_0 = 1.90$ F	$r_0 = 1.40$ F
$a = 0.827$ F	$a = 0.35$ F

^a A Saxon potential of the form $V(r) = -V_0/[1 + \exp(r-r_0)/a]$ was used for both the real and imaginary parts of the optical potential for both deuterons and neutrons.

TABLE III. Optical model parameters used for the DWBA calculations shown in Fig. 8.^a

Deuteron	Neutron
$V_0 = 84.5$ MeV	$V_0 = 43.0$ MeV
$W_0 = 22$ MeV	$W_0 = 6.45$ MeV
$r_0 = 1.33$ F	$r_0 = 1.40$ F
$a = 0.73$ F	$a = 0.35$ F
$r_w = 1.34$ F	
$a_w = 0.75$ F	

^a A Saxon potential $V(r) = V_0/[1 + \exp(r-r_0)/a]$ was used for the real part of the deuteron optical potential and for real and imaginary parts of the neutron optical potential. The imaginary part of the deuteron optical potential was given by a derivative potential of the form

$$W(r) = W_{ad}[1 + \exp(r-r_w)/a_w]/dr.$$

gave a reasonable fit to a portion of the elastic data of Seiler. Ambiguities in the depths of deuteron optical potentials have been noted previously,⁴⁴⁻⁴⁶ but the

⁴² S. Gorodetzky, P. Fintz, G. Bassompierre, and A. Gallmann, *Compt. Rend.* **252**, 713 (1961).

⁴³ R. F. Seiler, D. F. Herring, and K. W. Jones, *Bull. Am. Phys. Soc.* **8**, 304 (1963); and work to be published.

⁴⁴ E. C. Halbert, R. H. Bassel, and G. R. Satchler, *Bull. Am. Phys. Soc.* **7**, 357 (1962).

⁴⁵ R. M. Drisko, G. R. Satchler, and R. H. Bassel, *Phys. Letters* **5**, 347 (1963).

⁴⁶ C. M. Perey and F. G. Perey, *Phys. Rev.* **132**, 755 (1963).

other analyses do tend to favor the deeper well depths.⁴⁷⁻⁴⁹ The neutron optical potential was taken from the tabulation by J. R. Beyster *et al.*⁵⁰ A comparison of the distorted-wave Born-approximation calculations with the experimental results is shown in Figs. 7 and 8. The fits obtained with the deeper deuteron potential are clearly better than those obtained with the 20-MeV depth. The spectroscopic factor obtained by comparing the results of the distorted-wave calculation with the experimental cross sections was 0.15.

6. CONCLUSIONS

It was hoped at the start of the experiment that a measurement of the $N^{14}(d, n_0)O^{15}$ polarization might be of some help in determining the reaction mechanism. It is apparent that the present data can be reasonably accounted for on the basis of either compound nucleus or direct interaction mechanisms. An improvement in the accuracy of the experiment and data at other angles and energies would be helpful in distinguishing between the theoretical predictions made here, although further refinements in the theoretical computations involved would also be desirable. It does appear somewhat doubtful that polarization measurements will furnish a sensitive method of determining the reaction mechanism in the present case. Since the reaction mechanism is uncertain, it is not possible to extract any firm information about the level structure in O^{16} from this experiment.

⁴⁷ R. N. Maddison, Proc. Roy. Soc. (London) **79**, 264 (1962).

⁴⁸ W. R. Smith and E. V. Ivash, Phys. Rev. **131**, 304 (1963).

⁴⁹ P. E. Hodgson, *Direct Interactions and Nuclear Reaction Mechanisms* (Gordon and Breach Science Publishers, New York, 1963), p. 103.

⁵⁰ J. R. Beyster, R. G. Schrandt, M. Walt, and E. W. Salmi, LA-2099, 1956 (unpublished).

The properties of the $N^{14}(d, n_0)O^{15}$ reaction as a source of polarized 6.2-MeV neutrons are compared with the properties of other source reactions in Table IV. The best source is obviously the $T(p, n)He^3$ reac-

TABLE IV. Neutron source reactions for production of ~ 6.2 MeV polarized neutrons.

Source	Laboratory bombarding energy (MeV)	θ_{lab}	$\frac{d\sigma}{d\omega}$ (mb/sr) _{lab}	Polarization
$T(p, n)He^3$	8.1	40°	20 ^a	-0.20 ^b
$D(d, n)He^3$	3.8	35°	8°	-0.02 ^d
	4.1	40°	6°	-0.18 ^d
$N^{14}(d, n_0)O^{15}$	1.3	30°	2 ^e	+0.11
$Be^9(p, n_0)B^9$ †	8.6	50°	...	-0.18 ^g

^a W. E. Wilson, R. L. Walter, and D. B. Fossan, Nucl. Phys. **27**, 421 (1961).

^b R. L. Walter, W. Benenson, P. S. Dubbeldam, and T. H. May, Nucl. Phys. **30**, 292 (1962).

^c W. Haerberli, *Progress in Fast Neutron Physics* (The University of Chicago Press, Chicago, Illinois, 1963), p. 307.

^d The value of the polarization is not well established in this energy region.

^e Reference 3.

[†] Use of this reaction is difficult because of the presence of three-body breakup neutrons.

^g C. A. Kelsey, Nucl. Phys. **45**, 235 (1963).

tion, but it is possible that the $N^{14}(d, n_0)O^{15}$ reaction might be of some use to laboratories with accelerators that do not reach 8 MeV.

ACKNOWLEDGMENTS

We are indebted to H. C. Kim, V. A. Otte, and R. F. Seiler for their help with the experiment. We also wish to thank Dr. R. H. Bassel of Oak Ridge National Laboratory for his assistance with the distorted-wave computations.